MUSIC Algorithm for Imaging of Inhomogeneities Surrounded by Random Scatterers: Numerical Study

Won-Kwang Park

Abstract We consider an inverse scattering problem in which small dielectric inhomogeneities in two-dimensional space are surrounded by randomly distributed scatterers. We approach this problem using a Multiple Signal Classification (MUSIC) algorithm. This is motivated by the fact that collected Multi-static Response (MSR) matrix data can be represented as an asymptotic expansion formula in the presence of such inhomogeneities. The results obtained by numerical simulations show that MUSIC performs satisfactorily, even under conditions where a significant number of random scatterers affect the data.

1 Introduction

One of the main purposes of the inverse scattering problem is to find the locations of unknown inhomogeneities from scattered field data. This problem is challenging, owing to the its ill-posedness. However, it is an interesting problem as it arises in multiple fields, such as physics, medical science, and material engineering. Various detection algorithms have been suggested for approaching this problem, most being based on Newton-type iteration schemes. Related research can be found in [3, 13, 18, 24–27, 31, 37, 39, 42] and references therein. However, in order for such algorithms to be successfully applied, a good initial guess is required, which is close enough to the unknown object. Without this, one might suffer from large computational costs, with the risk of non-convergence issues. Moreover, these schemes require suitable regularization terms, which are highly dependent on the problem at hand; a priori information about unknown inhomogeneities; and the complex calculations of so-called Fréchet derivatives at each iteration step. Even if the above conditions are fulfilled, iteration schemes are very difficult to extend to multiple inhomogeneities.

W.-K. Park (✉)
Department of Mathematics, Kookmin University, 77 Jeongneung-ro,
Seongbuk-gu, Seoul 02707, South Korea
e-mail: parkwk@kookmin.ac.kr

Motivated by this difficulties, alternative noniterative algorithms have been successfully developed and applied to the various inverse problems, such as the MUltiple SIgnal Classification (MUSIC) [2, 4, 5, 7, 8, 15, 21, 22, 33, 35, 36, 43], linear sampling method [12, 14, 16, 17, 23], topological derivative [1, 9, 11, 13, 29, 30], and subspace migration algorithms [20, 28, 32, 34, 38]. Among these, MUSIC (MUltiple SIgnal Classification)-type algorithms have been successfully applied to the imaging of various types of inhomogeneities at fixed single frequency. However, their feasibility has only been confirmed for cases where the background medium is homogeneous. Therefore, the examination of the imaging performance of MUSIC when unknown inhomogeneities are surrounded by random scatterers presents an interesting research subject.

In this paper, we apply a MUSIC-type imaging algorithm to the detection of the locations of small dielectric inhomogeneities that are surrounded by dielectric random scatterers. This is based on the fact that the elements of the so-called Multi-Static Response (MSR) matrix can be represented by an asymptotic expansion formula, owing to the existence of inhomogeneities. For more details, we refer the reader to refer [4]. Using this property, we introduce a MUSIC-type imaging algorithm and perform various numerical simulations.

The rest of this paper is organized as follows. In Sect. 2, we briefly discuss the two-dimensional direct scattering problem and present an asymptotic expansion formula in the presence of small inhomogeneities. In Sect. 3, a MUSIC-type imaging functional is introduced. In Sect. 4, we present various results of numerical simulations, illustrating the effectiveness and limitations of MUSIC. A short conclusion follows in Sect. 5.

2 Direct Scattering Problem and Asymptotic Expansion Formula

In this section, we review a two-dimensional direct scattering problem and introduce an asymptotic expansion formula. For a more detailed description, we refer the reader to refer [4]. Let Σ_m, $m = 1, 2, \ldots, M$ be a dielectric inhomogeneity with a small diameter r_m, in the two-dimensional space $\mathbb{R}^2$. Throughout this paper, we assume that every Σ_m can be expressed as

$$\Sigma_m = \mathbf{z}_m + r_m \mathbf{B}_m,$$

where $\mathbf{z}_m$ denotes the location of Σ_m and $\mathbf{B}_m$ is a simply connected smooth domain containing the origin. For the sake, we let Σ be the collection of all Σ_m. Throughout this paper, we assume that inhomogeneities are well separated from each other, i.e., that there exists $d \in \mathbb{R}$ such that

$$0 < r \ll d \leq |\mathbf{z}_m - \mathbf{z}_{m'}|$$

for all $m, m' = 1, 2, \ldots, M$ and $m \neq m'$.

Let us denote Δ_s, $s = 1, 2, \ldots, S$, be the random scatterer with small a radius $r_s < r$, and let Δ be the collection of all Δ_s. Similarly to the above, we assume that Δ_s is of the form

$$\Delta_s = \mathbf{y}_s + r_s \mathbf{B}_s.$$

and $\Delta_s \cup \Delta_{s'} = \emptyset$ for all $s, s' = 1, 2, \ldots, S$ and $s \neq s'$.

In this paper, we assume that all inhomogeneities are characterized by their dielectric permittivity at a given positive angular frequency $\omega = 2\pi/\lambda$, where λ denotes the wavelength. Let ε_m, ε_s, and ε_0 be the electric permittivities of Σ_m, Δ_s, and $\mathbb{R}^2$, respectively. Then, we can introduce the piecewise-constant electric permittivity $\varepsilon(\mathbf{x})$, such that

$$\varepsilon(\mathbf{x}) = \begin{cases} \varepsilon_m & \text{for} \quad \mathbf{x} \in \Sigma_m, \\ \varepsilon_s & \text{for} \quad \mathbf{x} \in \Delta_s, \\ \varepsilon_0 & \text{for} \quad \mathbf{x} \in \mathbb{R}^2 \backslash (\bar{\Sigma} \cup \bar{\Delta}.) \end{cases}$$

For the sake of simplicity, we let $\varepsilon_0 = 1$ and $\varepsilon_m > \varepsilon_s$, for all m and s. Hence, we can set the wave number $k = \omega \sqrt{\varepsilon_0} = \omega$.

For a given fixed frequency ω, let

$$u_{\text{inc}}(\mathbf{x}, \boldsymbol{\theta}) = e^{i\omega \boldsymbol{\theta} \cdot \mathbf{x}}$$

be the plane-wave incident field with the incident direction $\boldsymbol{\theta} \in \mathbb{S}^1$, where $\mathbb{S}^1$ denotes a two-dimensional unit circle. Let $u(\mathbf{x}, \boldsymbol{\theta})$ denotes the time-harmonic total field that satisfies the Helmholtz equation

$$\triangle u(\mathbf{x}, \boldsymbol{\theta}) + \omega^2 \varepsilon(\mathbf{x}) u(\mathbf{x}, \boldsymbol{\theta}) = 0,$$

with transmission conditions on the boundaries of Σ_m and Δ_s. It is well known that $u(\mathbf{x}, \boldsymbol{\theta})$ can be decomposed as

$$u(\mathbf{x}, \boldsymbol{\theta}) = u_{\text{inc}}(\mathbf{x}, \boldsymbol{\theta}) + u_{\text{scat}}(\mathbf{x}, \boldsymbol{\theta}),$$

where $u_{\text{scat}}(\mathbf{x}, \boldsymbol{\theta})$ denotes the unknown scattered field that satisfies the Sommerfeld radiation condition

$$\lim_{|\mathbf{x}| \to 0} \sqrt{|\mathbf{x}|} \left(\frac{\partial u_{\text{scat}}(\mathbf{x}, \boldsymbol{\theta})}{\partial |\mathbf{x}|} - i\omega u_{\text{scat}}(\mathbf{x}, \boldsymbol{\theta}) \right) = 0$$

uniformly in all directions $\boldsymbol{\vartheta} = \frac{\mathbf{x}}{|\mathbf{x}|} \in \mathbb{S}^1$. The far-field pattern $u_\infty(\boldsymbol{\vartheta}, \boldsymbol{\theta})$ of the scattered field $u_{\text{scat}}(\mathbf{x}, \boldsymbol{\theta})$ is defined on $\mathbb{S}^1$. It can be expressed as

$$u_{\text{scat}}(\mathbf{x}, \boldsymbol{\theta}) = \frac{e^{i\omega|\mathbf{x}|}}{\sqrt{|\mathbf{x}|}} u_\infty(\boldsymbol{\vartheta}, \boldsymbol{\theta}) + o\left(\frac{1}{\sqrt{|\mathbf{x}|}}\right), \quad |\mathbf{x}| \to +\infty.$$

Then, by virtue of result in [10], the far-field pattern $u_\infty(\boldsymbol{\vartheta}, \boldsymbol{\theta})$ can be written using the following asymptotic expansion formula, which plays a key role in the MUSIC-type algorithm that will be designed in the next section:

$$\begin{aligned} u_\infty(\boldsymbol{\vartheta}, \boldsymbol{\theta}) = \frac{\omega^2(1+i)}{4\sqrt{\omega\pi}} &\left(\sum_{m=1}^{M} r_m^2(\varepsilon_m - \varepsilon_0)|\mathbf{B}_m|e^{i\omega(\boldsymbol{\theta}-\boldsymbol{\vartheta})\cdot\mathbf{z}_m} \right. \\ &\left. + \sum_{s=1}^{S} r_s^2(\varepsilon_s - \varepsilon_0)|\mathbf{B}_s|e^{i\omega(\boldsymbol{\theta}-\boldsymbol{\vartheta})\cdot\mathbf{y}_s} \right). \end{aligned} \tag{1}$$

3 MUSIC-type Imaging Algorithm

In this section, we introduce a MUSIC-type algorithm for detecting the locations of small inhomogeneities. For the sake of simplicity, we exclude the constant term $\frac{\omega^2(1+i)}{4\sqrt{\omega\pi}}$ from (1). To proceed, let us consider the eigenvalue structure of the MSR matrix

$$\mathbb{K} = \begin{bmatrix} u_\infty(\boldsymbol{\vartheta}_1, \boldsymbol{\theta}_1) & u_\infty(\boldsymbol{\vartheta}_1, \boldsymbol{\theta}_2) & \cdots & u_\infty(\boldsymbol{\vartheta}_1, \boldsymbol{\theta}_N) \\ u_\infty(\boldsymbol{\vartheta}_2, \boldsymbol{\theta}_1) & u_\infty(\boldsymbol{\vartheta}_2, \boldsymbol{\theta}_2) & \cdots & u_\infty(\boldsymbol{\vartheta}_2, \boldsymbol{\theta}_N) \\ \vdots & \vdots & \ddots & \vdots \\ u_\infty(\boldsymbol{\vartheta}_N, \boldsymbol{\theta}_1) & u_\infty(\boldsymbol{\vartheta}_N, \boldsymbol{\theta}_2) & \cdots & u_\infty(\boldsymbol{\vartheta}_N, \boldsymbol{\theta}_N) \end{bmatrix}.$$

Suppose that $\boldsymbol{\vartheta}_j = -\boldsymbol{\theta}_j$ for all j. Then, $\mathbb{K}$ is a complex symmetric matrix, but is not Hermitian. Therefore, instead of Eigenvalue decomposition, we perform singular value decomposition (SVD) on $\mathbb{K}$ (see [16]):

$$\mathbb{K} \approx \sum_{m=1}^{M} \sigma_m \mathbf{U}_m \mathbf{V}_m^* + \sum_{s=M+1}^{M+S} \sigma_s \mathbf{U}_s \mathbf{V}_s^*, \tag{2}$$

where the superscript $*$ is used to denote the Hermitian. Then, $\{\mathbf{U}_1, \mathbf{U}_2, \ldots, \mathbf{U}_{M+S}\}$ is an orthogonal basis for the signal space of $\mathbb{K}$. Therefore, one can define the

projection operator onto the null (or noise) subspace, $\mathbf{P}_{\text{noise}} : \mathbb{C}^{N \times 1} \to \mathbb{C}^{N \times 1}$. This projection is given explicitly by

$$\mathbf{P}_{\text{noise}} := \mathbb{I}_N - \sum_{m=1}^{M+S} \mathbf{U}_m \mathbf{U}_m^*, \tag{3}$$

where $\mathbb{I}_N$ denotes the $N \times N$ identity matrix. For any point $\mathbf{x} \in \mathbb{R}^2$, we define a test vector $\mathbf{f}(\mathbf{x}) \in \mathbb{C}^{N \times 1}$ as

$$\mathbf{f}(\mathbf{x}) = \frac{1}{N} [e^{i\omega\theta_1 \cdot \mathbf{x}}, e^{i\omega\theta_2 \cdot \mathbf{x}}, \ldots, e^{i\omega\theta_N \cdot \mathbf{x}}]^T.$$

Then, by virtue of [4], there exists an $N_0 \in \mathbb{N}$ such that for any $N \geq N_0$, the following statement holds:

$$\mathbf{f}(\mathbf{x}) \in \text{Range}(\mathbb{K}\bar{\mathbb{K}}) \quad \text{if and only if } \mathbf{x} \in \Sigma_m \text{ or } \mathbf{x} \in \Delta_s,$$

for $m = 1, 2, \ldots, M$ and $s = 1, 2, \ldots, S$. This means that if $\mathbf{x} \in \Sigma_m$ or $\mathbf{x} \in \Delta_s$, then

$$|\mathbf{P}_{\text{noise}}(\mathbf{f}(\mathbf{x}))| = 0.$$

Thus, the locations of Σ_m and Δ_s follow from computing the MUSIC-type imaging function

$$\mathcal{I}(\mathbf{x}) = \frac{1}{|\mathbf{P}_{\text{noise}}(\mathbf{f}(\mathbf{x}))|}. \tag{4}$$

The resulting plot of $\mathcal{I}(\mathbf{x})$ will have peaks of large magnitudes at $\mathbf{z}_m \in \Sigma_m$ and $\mathbf{y}_s \in \Delta_s$.

Remark 3.1 If the size or permittivity of Δ_s is sufficiently small such that either $r_s \ll r_m$ or $\varepsilon_s \ll \varepsilon_m$, for all $m = 1, 2, \ldots, M$ and $s = 1, 2, \ldots, S$, then the values of the singular value σ_s can be negligible. In this case, the locations of the Δ_s cannot be detected via the map of $\mathcal{I}(\mathbf{x})$. If neither the size nor the permittivity of Δ_s is that small, then σ_s cannot be negligible, i.e., the locations of Δ_s will be detected via the map of $\mathcal{I}(\mathbf{x})$.

4   Results of Numerical Simulations

In this section, the results of some numerical simulations are exhibited in order to examine the imaging performance of MUSIC. The radii of all Σ_m and Δ_s are set to 0.1 and 0.03 (or 0.05), respectively, and permittivities of Δ_s are selected as random values between 1 and 2. For the incident (and observation) directions, we set

$$\boldsymbol{\theta}_j = -\left[\cos\frac{2\pi(j-1)}{N}, \frac{2\pi(j-1)}{N}\right]^T.$$

The corresponding test configuration is shown in Table 1, and distribution of three inhomogeneities and random scatterers is presented in Fig. 1.

It is worth emphasizing that the dataset of the MSR matrix $\mathbb{K}$ is generated by means of the Foldy-Lax framework in order to avoid *inverse crime*. For more details, we refer the reader to refer [38, 41]. After the generation, the singular value decomposition of $\mathbb{K}$ is performed via the MATLAB command 'svd.' In order to distinguish nonzero singular values of $\mathbb{K}$, a 0.1-threshold scheme is applied, i.e., choosing the first j singular values σ_j such that $\frac{\sigma_j}{\sigma_1} \geq 0.1$. For a more detailed description, we refer the reader to refer [35, 36].

Figure 2 shows the distribution of the normalized singular values of $\mathbb{K}$ and map of $\mathcal{I}(\mathbf{x})$ under setting 1. Because the radius and the permittivities of the random scatterers are small, the three nonzero singular values are successfully determined, so one can detect the locations of the Σ_m exactly.

Figure 3 shows the distribution of the normalized singular values of $\mathbb{K}$ and map of $\mathcal{I}(\mathbf{x})$ under setting 2. Although some artifacts are included in the map of $\mathcal{I}(\mathbf{x})$, the locations of the Σ_m are successfully identified.

Table 1 Test configuration

Settings	Value of N	Value of λ	Value of ε_m	Value of r_s
Setting 1	32	0.5	5	0.03
Setting 2	48	0.2	5	0.03
Setting 3	48	0.4	3	0.05
Setting 4	128	0.2	3	0.05

Fig. 1 Distribution of inhomogeneities (*red-colored circle*) and random scatterers (*blue-colored '×' mark*)
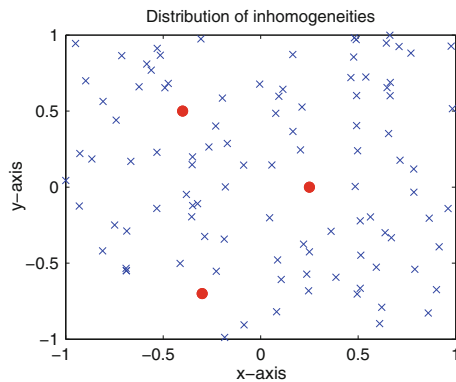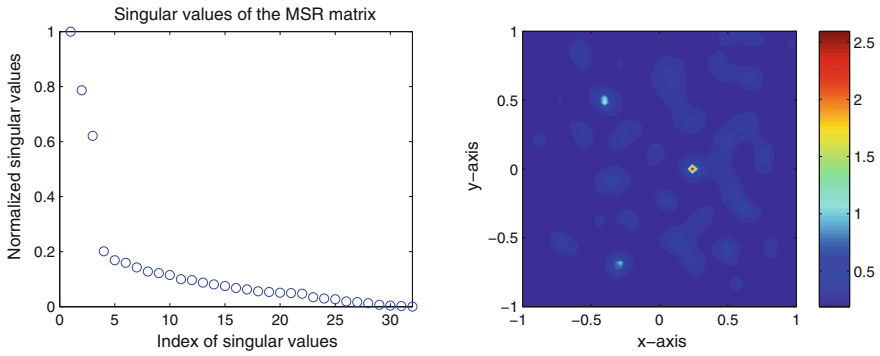
Fig. 2 Distribution of normalized singular values (*left*) and map of $\mathcal{I}(\mathbf{x})$ (*right*) under setting 1 configuration
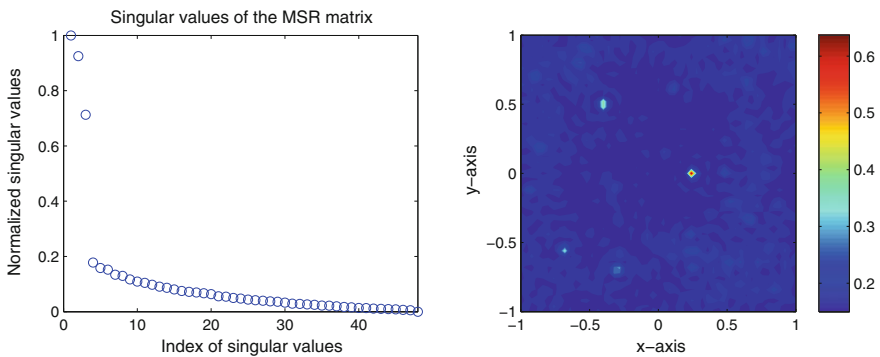

Fig. 3 Similar to Fig. 2, except under setting 2 configuration

Note that if the values $|\varepsilon_m - \varepsilon_s|$ and $|r_m - r_s|$ are small, then the σ_s is no longer negligible. This means that the locations of the Δ_s will be identified in the map of $\mathcal{I}(\mathbf{x})$, and this will disturb the identification of the Σ_m. This is evident in Fig. 4.

For the final example, let us consider the results in Fig. 5. Although N is sufficiently large and the value of λ is sufficiently small, it is very difficult to identify the true locations of the Σ_m.

Based on Figs. 2, 3, 4, and 5, we can conclude that MUSIC is an effective detection technique when the values of the permittivity and the radii of random scatterers are small compared to those of the inhomogeneities. On the other hand, as in the case of our settings 3 and 4, a method of improvement is highly necessary.
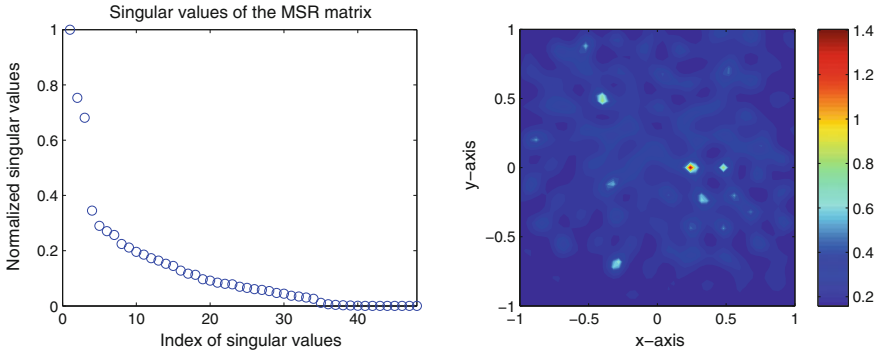
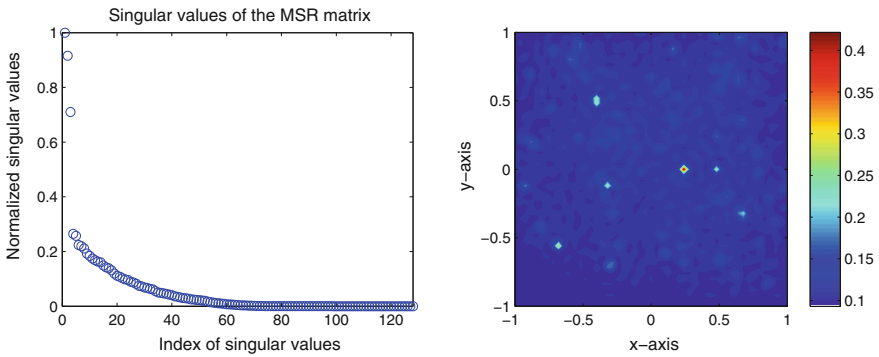**Fig. 4** Similar to Fig. 2, except under setting 3 configuration

Fig. 5 Similar to Fig. 2, except under setting 4 configuration

5 Conclusion

In this paper, we have considered a MUSIC-type imaging algorithm that is based on an asymptotic expansion formula in the presence of small inhomogeneities and random scatterers. Furthermore, the imaging performance of this MUSIC-type algorithm has been considered when small inhomogeneities are surrounded by random scatterers. Through numerical results, we have observed that MUSIC is an effective technique for identifying inhomogeneities when the random scatterers can be considered negligible, but still required an improvement when the random scatterers cannot be neglected.

In this paper, we focused on the numerical study of MUSIC. A mathematical analysis of the MUSIC-type imaging functional will be considered in future research, by establishing a relationship with Bessel functions of integer order of first kind. We expect that this analysis will illuminate some theoretical properties of MUSIC and suggest some methods of improvements.

Presently, we have considered a purely dielectric case. However, it could be extended to the contrasting purely magnetic case. Moreover, based on the mathematical treatment of the asymptotic formula, the imaging algorithm could be extended to a three-dimensional problem. For more details, we refer the reader to refer [6, 19, 40].

References

1. Ahn CY, Jeon K, Ma YK, Park WK (2014) A study on the topological derivative-based imaging of thin electromagnetic inhomogeneities in limited-aperture problems. Inverse Prob 30:105004
2. Ahn CY, Jeon K, Park WK (2015) Analysis of MUSIC-type imaging functional for single, thin electromagnetic inhomogeneity in limited-view inverse scattering problem. J Comput Phys 291:198–217
3. Àlvarez D, Dorn O, Irishina N, Moscoso M (2009) Crack reconstruction using a level-set strategy. J Comput Phys 228:5710–5721
4. Ammari H, Kang H (2004) Reconstruction of small Inhomogeneities from boundary measurements. Lecture notes in mathematics, vol 1846. Springer, Berlin
5. Ammari H, Iakovleva E, Lesselier D (2005) A MUSIC algorithm for locating small inclusions buried in a half-space from the scattering amplitude at a fixed frequency. Multiscale Model Simul 3:597–628
6. Ammari H, Iakovleva E, Lesselier D, Perrusson G (2007) MUSIC type electromagnetic imaging of a collection of small three-dimensional inclusions. SIAM J Sci Comput 29: 674–709
7. Ammari H, Kang H, Lee H, Park WK (2010) Asymptotic imaging of perfectly conducting cracks. SIAM J Sci Comput 32:894–922
8. Ammari H, Garnier J, Kang H, Park WK, Sølna K (2011) Imaging schemes for perfectly conducting cracks. SIAM J Appl Math 71:68–91
9. Ammari H, Garnier J, Jugnon V, Kang H (2012) Stability and resolution analysis for a topological derivative based imaging functional. SIAM J Control Optim 50:48–76
10. Beretta E, Francini E (2003) Asymptotic formulas for perturbations of the electromagnetic fields in the presence of thin imperfections. Contemp Math 333:49–63
11. Burger M, Hackl B, Ring W (2004) Incorporating topological derivatives into level-set methods. J Comput Phys 194:344–362
12. Cakoni F, Colton D (2003) The linear sampling method for cracks. Inverse Prob 19:279–295
13. Carpio A, Rapun ML (2008) Solving inhomogeneous inverse problems by topological derivative methods. Inverse Prob 24:045014
14. Charalambopoulos A, Gintides D, Kiriaki K (2002) The linear sampling method for the transmission problem in three-dimensional linear elasticity. Inverse Prob 18:547–558
15. Chen X, Zhong Y (2009) MUSIC electromagnetic imaging with enhanced resolution for small inclusions. Inverse Prob 25:015008
16. Cheney M (2001) The linear sampling method and the MUSIC algorithm. Inverse Prob 17:591–595
17. Colton D, Haddar H, Monk P (2002) The linear sampling method for solving the electromagnetic inverse scattering problem. SIAM J Sci Comput 24:719–731

18. Dorn O, Lesselier D (2006) Level set methods for inverse scattering. Inverse Prob 22: R67–R131
19. Gdoura S, Lesselier D, Chaumet PC, Perrusson G (2009) Imaging of a small dielectric sphere buried in a half space. ESAIM Proc 26:123–134
20. Hou S, Huang K, Sølna K, Zhao H (2009) A phase and space coherent direct imaging method. J Acoust Soc Am 125:227–238
21. Joh YD, Park WK (2013) Structural behavior of the MUSIC-type algorithm for imaging perfectly conducting cracks. Prog Electromagn Res 138:211–226
22. Joh YD, Kwon YM, Park WK (2014) MUSIC-type imaging of perfectly conducting cracks in limited-view inverse scattering problems. Appl Math Comput 240:273–280
23. Kirsch A, Ritter S (2000) A linear sampling method for inverse scattering from an open arc. Inverse Prob 16:89–105
24. Kress R (1995) Inverse scattering from an open arc. Math Methods Appl Sci 18:267–293
25. Kress R, Serranho P (2005) A hybrid method for two-dimensional crack reconstruction. Inverse Prob 21:773–784
26. Kress R, Serranho P (2007) A hybrid method for sound-hard obstacle reconstruction. J Comput Appl Math 204:418–427
27. Mönch L (1996) On the numerical solution of the direct scattering problem for an open sound-hard arc. J Comput Appl Math 17:343–356
28. Park WK (2010) On the imaging of thin dielectric inclusions buried within a half-space. Inverse Prob 26:074008
29. Park WK (2012) Topological derivative strategy for one-step iteration imaging of arbitrary shaped thin, curve-like electromagnetic inclusions. J Comput Phys 231:1426–1439
30. Park WK (2013) Multi-frequency topological derivative for approximate shape acquisition of curve-like thin electromagnetic inhomogeneities. J Math Anal Appl 404:501–518
31. Park WK (2013) Shape reconstruction of thin electromagnetic inclusions via boundary measurements: level-set method combined with topological derivative. Math Probl Eng 2013:125909
32. Park WK (2014) Analysis of a multi-frequency electromagnetic imaging functional for thin, crack-like electromagnetic inclusions. Appl Numer Math 77:31–42
33. Park WK (2015) Asymptotic properties of MUSIC-type imaging in two-dimensional inverse scattering from thin electromagnetic inclusions. SIAM J Appl Math 75:209–228
34. Park WK (2015) Multi-frequency subspace migration for imaging of perfectly conducting, arc-like cracks in full- and limited-view inverse scattering problems. J Comput Phys 283:52–80
35. Park WK, Lesselier D (2009) Electromagnetic MUSIC-type imaging of perfectly conducting, arc-like cracks at single frequency. J Comput Phys 228:8093–8111
36. Park WK, Lesselier D (2009) MUSIC-type imaging of a thin penetrable inclusion from its far-field multi-static response matrix. Inverse Prob 25:075002
37. Park WK, Lesselier D (2009) Reconstruction of thin electromagnetic inclusions by a level set method. Inverse Prob 25:085010
38. Park WK, Lesselier D (2012) Fast electromagnetic imaging of thin inclusions in half-space affected by random scatterers. Waves Random Complex Media 22:3–23
39. Santosa F(1996) A level-set approach for inverse problems involving obstacles. ESAIM Control Optim Calc Var 1:17–33
40. Song R, Chen R, Chen X (2012) Imaging three-dimensional anisotropic scatterers in multi-layered medium by MUSIC method with enhanced resolution. J Opt Soc Am A 29:1900–1905
41. Tsang L, Kong JA, Ding KH, Ao CO (2001) Scattering of Electromagnetic Waves: Numerical Simulations. John Wiley, New York
42. Ventura G, Xu JX, Belytschko T (2002) A vector level set method and new discontinuity approximations for crack growth by EFG. Int J Numer Methods Eng 54:923–944
43. Zhong Y, Chen X (2007) MUSIC imaging and electromagnetic inverse scattering of multiple-scattering small anisotropic spheres. IEEE Trans Antennas Propag 55:3542–3549